

# LAMINAR FILM CONDENSATION ON HELICAL REFLUX CONDENSERS AND RELATED CONFIGURATIONS

AMIR KARIMI

Boiling and Phase Change Laboratory, Mechanical Engineering Department,  
University of Kentucky, Lexington, KY 40506, U.S.A.

(Received 11 May 1976 and in revised form 3 December 1976)

**Abstract**—Laminar film condensation on helical elliptical cylinders is analyzed using the Nusselt-Rohsenow method. The formulation includes both local centrifugal and gravitational forces. A general dimensionless differential equation is presented and dimensionless centrifugal and configuration parameters are identified. A variety of condensing systems, in particular various semi-infinite helical circular cylinders, are treated. Finally, heat-transfer results are presented and discussed. In all practical situations (excluding liquid metal condensation) the average heat-transfer coefficients for condensation on semi-infinite helical circular cylinders, lie within 8.5% of values for inclined circular cylinders.

## NOMENCLATURE

$A, a, b$ ,  $\equiv \mu k \Delta T / (\rho_f - \rho_g) \rho_f h'_{fg}$ ;  
horizontal and vertical semi-axes of an ellipse respectively;

$B$ ,  $\equiv$  dimensionless centrifugal parameter,  
equal to  $\left( \frac{\rho_f - \rho_g}{\rho_f} \right) \left( \frac{C_p \Delta T}{h'_{fg}} \right) \tan^2 \alpha / Pr$ ;

$C_p$ , specific heat of condensate;

$d$ , diameter of circular cylinder, or sphere;

$D$ , diameter of helix, equal to  $2R$ ;

$F$ ,  $\equiv \overline{Nu}_L / [gL^3/A]^{1/4}$ ;

$g$ , gravitational acceleration;

$g_{x_1}, g_{\phi}$ , axial and polar components of gravitational acceleration, respectively;

$G, G_{\phi}$ , resultant and polar component of local effective acceleration, respectively;

$h$ , local heat-transfer coefficient;

$\bar{h}$ , average heat-transfer coefficient,  
 $\frac{1}{A} \int_A h dA$ ;

$h_{fg}$ , latent heat of vaporization;

$h'_{fg}$ ,  $h_{fg}$ , corrected to account for sensible heat of subcooling in the film, equal to  $h_{fg} + 0.68 C_p \Delta T$ ;

$k$ , thermal conductivity of condensate;

$L$ , characteristic length ( $d$  for horizontal cylinder,  $d/\cos \alpha$  for inclined cylinder, etc.);

$\overline{Nu}_L$ , average Nusselt number,  $\frac{\bar{h}L}{k}$ ;

$Pr$ , Prandtl number;

$r$ , radius of circular cylinder, or sphere;

$R$ , radius of helix;

$\bar{R}$ , a distance from the center of helix to a point on the surface of the helical cylinder;

$V_m$ , average local velocity in direction of flow;

$(V_{axial})_m$ , average local axial velocity;

$x_1, x_2, x_3$ , coordinate axis of a helical cylinder;

$X$ , reduced axial distance, equal to  $x_1/b \tan \alpha$  for sloping elliptical cylinders, and  $2x_1/d \tan \alpha$  for sloping circular cylinders;

$Z$ ,  $\equiv$  dimensionless group representing the film thickness, equal to  $\left( \frac{g \cos \alpha \delta^4}{3bA} \right)$ .

## Greek symbols

$\dot{m}$ , mass flow rate of condensate;

$\alpha$ , helix angle, or angle of inclination;

$\beta$ , polar angle of the upper stagnation point in  $x_1$  plane, Fig. 5;

$\beta_{max}$ , polar angle indicating the location of maximum film thickness on the cylinder, Fig. 5;

$\Delta T$ , difference between saturation temperature and wall temperature ( $T_{sv} - T_0$ );

$\delta$ , condensate film thickness;

$\bar{\gamma}$ , polar angle in cylindrical coordinates;

$\bar{\gamma}/\cos \alpha$ ;

$\phi$ , polar angle in  $x_1$  plane;

$\rho_f, \rho_g$ , densities of liquid and saturated vapor respectively;

$\psi$ , angle between momentary path of condensate and constant  $x_1$  lines;

$\mu$ , viscosity of condensate;

$\omega^2 \bar{R}$ , local centrifugal acceleration;

$(\omega^2 \bar{R})_{\phi}$ , polar component of local centrifugal acceleration.

## INTRODUCTION

THE PROCESS of laminar film condensation on a number of systems (flat plates, cylinders, spheres, etc.) has been extensively studied. However, heat is frequently removed by condensation on the surface of helical reflux condensers, and that configuration appears not to have been analyzed. Experimental obser-

vations of condensation on the surface of helical reflux condensers reveal the effect of centrifugal forces on the condensate. It is observed that condensate droplets are flung downward and outward from the helix.\* The present investigation treats condensation on helical circular cylinders, taking into consideration the induced centrifugal forces.

The original analysis of the problem of film condensation on a vertical flat plate in a constant gravity field was done by Nusselt [1] in 1916. Since then, a number of investigators have made significant improvements on the Nusselt theory.

Bromley [2] considered the effects of subcooling, dropping Nusselt's assumption of a linear temperature distribution. Rohsenow [3] presented a modified integral analysis which removed some of Bromley's approximations. In his analysis Rohsenow shows that for a range of  $0 < C_p \Delta T / h_{fg} < 1.0$  the average Nusselt number for laminar film condensation on a vertical plate, based on the length of the plate,  $L$ , very closely approximates to

$$\overline{Nu}_L = 0.943 \left[ \frac{gL^3}{A} \right]^{1/4} \quad (1)$$

where

$$A \equiv \mu k \Delta T / \rho_f (\rho_f - \rho_g) h'_{fg}$$

and

$$h'_{fg} = h_{fg} (1 + 0.68 C_p \Delta T / h_{fg}).$$

The adequacy of the simple Nusselt-Rohsenow theory in practical situations has been well established. Sparrow and Gregg's [4, 5] boundary-layer treatment of isothermal vertical plates and horizontal cylinders, and Chen [6] and Koh *et al.*'s [7] consideration of the effect of the vapor drag exerted on the liquid film, proved the accuracy of the simple theory as long as the Prandtl number,  $Pr$ , was on the order of unity or greater and  $C_p \Delta T / h_{fg}$  was less than unity.

Hassan and Jakob [8] considered laminar film condensation on circular cylinders of radius,  $r$ , inclined with an angle,  $\alpha$ , from the horizontal. They assumed that the velocity distribution at a point on the surface of the cylinder is the same as that on a fully developed film flowing on a plane tangent to the surface at that point. Their results showed that the condensate thickness approaches a limiting value so long as  $X > 3.2$ , where  $X$  is the axial distance from the leading edge of the cylinder divided by  $r \tan \alpha$ . Hassan and Jakob also showed that the dimensionless length of the cylinder,  $X$ , has to be greater than or equal to 50 so that the heat-transfer coefficient value averaged over the entire surface of the cylinder approaches that of an infinitely long cylinder. This effect results from the fact that the film is thin in the starting region of the cylinder ( $X < 3.2$ ). †

\*This action was observed very clearly in the large reflux condenser built by Lienhard and Dhir for their flat-plate boiling experiment in this laboratory.

†For most practical situations  $X = 50$  is relatively small, e.g. only 8.5 cm of a 13 mm O.D. cylinder inclined  $15^\circ$  from the horizontal is required to reach the value of  $X = 50$ .

By adopting these modifications of Nusselt's assumptions, we can develop an analysis of laminar film condensation on the very general configuration of a helical elliptical cylinder. This analysis will be based on the restrictions that the Prandtl number is not much less than unity; the ratio of sensible to latent heat  $C_p \Delta T / h_{fg} \leq 1.0$ ; and no liquid is added by dripping from the adjacent upper level of tubing. (It will be shown that for limiting geometrical configurations this restriction is satisfied.) We shall also assume that at each point on the surface of the condenser, the components of the forces exerted on the condensate follow the Nusselt assumption of static balance of forces, enabling us to lump the components of gravitational and local centrifugal acceleration together at each point on the surface of the condenser. As in all of the previous condensation solutions, the solution will apply to surfaces with a radius of curvature much greater than the film thickness. Finally, this solution will be applied to the common case of a circular helical cylinder.

#### ANALYSIS

A helical cylinder with an elliptical cross section, helix angle,  $\alpha$ , and helix radius,  $R$ , is shown in Fig. 1.  $R$  is the distance between the centers of the helix and cylinder.

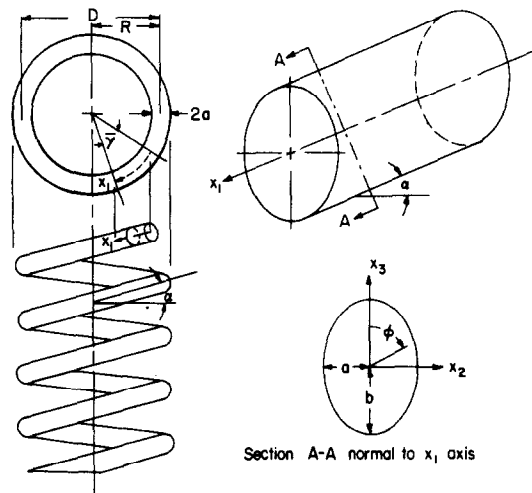


FIG. 1. Helical elliptical cylinders and coordinate axes.

The length of a helix of radius  $R$  and angle  $\alpha$  is equal to  $R\bar{\gamma}/\cos \alpha$ , where  $\bar{\gamma}$  is the polar angle in a cylindrical coordinate representing the center of the helical cylinder. Hence the helical cylinder under consideration can be presented in the following form:

$$\begin{aligned} x_1 &= \bar{R}(\phi)\gamma \\ x_2 &= a \sin \phi \\ x_3 &= b \cos \phi \end{aligned} \quad (2)^*$$

where  $\gamma = \bar{\gamma}/\cos \alpha$ ,  $\phi$  is an angle of the polar coordinate system in the  $x_1$  plane, and

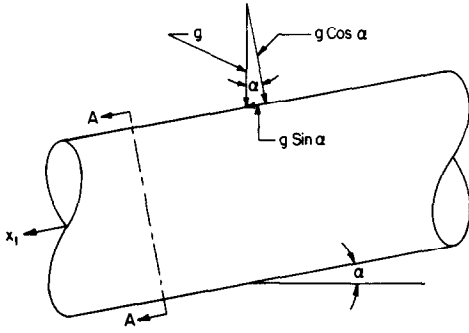
$$\bar{R}(\phi) = R \left( 1 + \frac{a}{R} \sin \phi \right). \quad (3)$$

\* $0 \leq \phi \leq \pi$  represents the outer half, and  $\pi \leq \phi \leq 2\pi$  the inner half, of the helical cylinder.

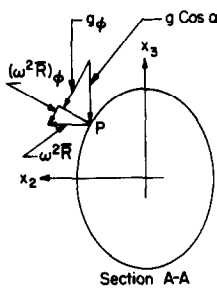
**Effective acceleration**

The gravitational acceleration acting on the cylinder can be resolved into two components as shown in Fig. 2(a). At all points on the cylinder the component of the gravity,

$$g_{x_1} = g \sin \alpha \tag{4}$$



a) Gravitational components



b) Polar gravitation and centrifugal components

FIG. 2. Effective acceleration.

is the only acceleration acting on the condensate film in the axial direction. However, there are two modes of acceleration, gravitational and centrifugal, acting on the condensate film in the polar direction as shown in Fig. 2(b). The polar gravitational component is expressible as

$$g_\phi = g \frac{\sin \phi \cos \alpha}{[E(\phi)]^{1/2}} \tag{5}$$

where

$$E(\phi) = \sin^2 \phi + \left(\frac{a}{b}\right)^2 \cos^2 \phi.$$

The local centrifugal acceleration  $\omega^2 \bar{R}(\phi)$  is defined as

$$\omega^2 \bar{R}(\phi) = \frac{(V_{axial})_m^2}{\bar{R}(\phi)} \tag{6}$$

where  $\omega$  is the angular velocity and  $\bar{R}(\phi)$  is the local radius of the helix at a point  $P$  on the cylinder. The polar component of the local centrifugal acceleration

acting on the condensate film as shown in Fig. 2(b) can be presented as

$$[\omega^2 \bar{R}(\phi)]_\phi = \frac{a (\rho_f - \rho_g)^2 \delta^4 g_{x_1}^2 \cos \phi}{b 9\mu^2 \bar{R}(\phi) [E(\phi)]^{1/2}}. \tag{7}$$

Therefore, the local effective acceleration,  $G$ , acting on the condensate film can be expressed as

$$G = [g_{x_1}^2 + G_\phi^2]^{1/2} \tag{8}$$

where

$$G_\phi = g_\phi + [\omega^2 \bar{R}(\phi)]_\phi.$$

The magnitude of the axial gravitational acceleration  $g_{x_1}$  is constant. However, the magnitude of  $G_\phi$  varies with the local film thickness. Hence the magnitude and direction of the effective gravity,  $G$ , varies continuously with the variation of the local condensate film thickness on the cylinder.

Nusselt's local average film velocity,  $V_m$ , is expressible in terms of the film thickness  $\delta(x_1, \phi)$  and  $G$  without reference to the history of the film up to this location, as

$$V_m = \frac{(\rho_f - \rho_g) \delta^2}{3\mu} G. \tag{9}$$

**GOVERNING DIFFERENTIAL EQUATION**

Consider the volume element shown in Fig. 3. The condensate with an average velocity  $V_m$  tangent to the surface of cylinder flows into the element.  $V_m$  makes

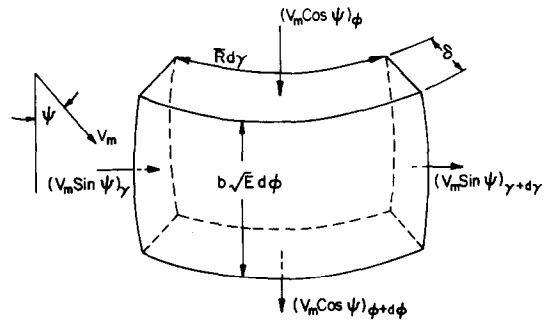


FIG. 3. Volume element.

an angle  $(\pi/2) - \psi$  with the normal to  $x_1$  plane, where

$$\psi = \sin^{-1} \frac{g_{x_1}}{G} = \cos^{-1} \frac{G_\phi}{G}. \tag{10}$$

The rate of heat lost by vapor condensing on the volume element is equal to the rate of heat transfer by conduction through the film. Hence with the aid of the continuity relation, the following is developed

$$\frac{k}{\delta} b [E(\phi)]^{1/2} \bar{R}(\phi) \Delta T = \rho_f h_{fg} \left\{ \frac{\partial}{\partial \phi} [V_m \cos \psi \delta \bar{R}(\phi)] + \frac{\partial}{\partial \gamma} [V_m \sin \psi b [E(\phi)]^{1/2} \delta] \right\}. \tag{11}$$

Substituting equations (3), (9) and (10) and rearranging (11) give

$$\frac{3Ab(1+a \sin \phi/R)}{\cos \alpha} = \left[ \frac{\cos \phi(1+2a \sin \phi/R)}{E(\phi)} - \frac{(1-a^2/b^2) \sin^2 \phi \cos \phi(1+a \sin \phi/R)}{[E(\phi)]^2} \right] \delta^4 - \frac{a(\rho_f - \rho_g)^2 \sin^2 \alpha}{b \cdot 9\mu^2 R \cos \alpha} \left[ \frac{\sin \phi}{E(\phi)} - \frac{(1-a^2/b^2) \cos^2 \phi \sin \phi}{[E(\phi)]^2} \right] \delta^8 + 3 \frac{\sin \phi(1+a \sin \phi/R)}{E(\phi)} \delta^3 \frac{\partial \delta}{\partial \phi} + 7 \left[ \frac{(a/b)(\rho_f - \rho_g)^2 g \sin^2 \alpha}{9\mu^2 R \cos \alpha} \right] \frac{\cos \phi \delta^7}{E(\phi)} \frac{\partial \delta}{\partial \phi} + 3\delta^3 \tan \alpha b \frac{\partial \delta}{\partial x_1}. \tag{12}$$

Introducing the dimensionless groups:

$$Z \equiv \frac{g \cos \alpha \delta^4}{3bA}; \quad X \equiv \frac{x_1}{b \tan \alpha}$$

we can express equation (10)

$$\frac{\partial Z}{\partial X} + \frac{1}{E(\phi)} \left[ \sin \phi \left( 1 + \frac{a}{R} \sin \phi \right) + \frac{7}{9} B \frac{a}{R} (\cos \phi) Z \right] \frac{\partial Z}{\partial \phi} + \frac{4}{3} \left[ \frac{\cos \phi(1+2a \sin \phi/R)}{E(\phi)} - \frac{(1-a^2/b^2) \sin^2 \phi \cos \phi(1+a \sin \phi/R)}{[E(\phi)]^2} \right] Z - \frac{4}{9} B \frac{a}{R} \left[ \frac{\sin \phi}{E(\phi)} - \frac{(1-a^2/b^2) \cos^2 \phi \sin \phi}{[E(\phi)]^2} \right] Z^2 = \frac{4}{3} \left( 1 + \frac{a}{R} \sin \phi \right) \tag{13}$$

where

$$B \equiv \left( \frac{\rho_f - \rho_g}{\rho_f} \right) \left( \frac{C_p \Delta T}{h'_{fg}} \right) \tan^2 \alpha / Pr. \tag{14}$$

Equation (13) is subject to the boundary condition

$$Z(X=0, \phi) = 0. \tag{15}$$

Finally, the average Nusselt number is defined as

$$\overline{Nu}_L = \frac{\bar{h}L}{k} \tag{16}$$

where  $L$  represents a characteristic length, and  $\bar{h}$  is the average heat-transfer coefficient, readily obtainable by averaging the local heat-transfer coefficient

$$h(X, \phi) = \frac{k}{\delta} = \left( \frac{g \rho_f (\rho_f - \rho_g) h'_{fg} k^3 \cos \alpha}{3b\mu \Delta T Z(X, \phi)} \right)^{1/4} \tag{17}$$

over the entire surface of the cylinder.

Equation (13) relates the dimensionless group,  $Z$ , and in turn the film thickness,  $\delta$ , with the configuration parameters  $a/R$ ,  $a/b$ , and the centrifugal parameter  $B$ . The non-linear terms in equation (13) are a result of the centrifugal forces exerted on the condensate film. An interesting observation is the fact that the non-linear terms in equation (13) are eliminated for either diminishing values of  $B$ , or  $a/R$ . Hence modification of the governing differential equation of laminar film condensation on a helical cylinder with an elliptical cross section [equations (12) or (13)] will result in the following cases.

1. *Inclined elliptical and circular cylinders*

For  $R = \infty$ , the differential equation (13) reduces to

$$\frac{\partial Z}{\partial X} + \frac{\sin \phi}{E(\phi)} \frac{\partial Z}{\partial \phi} + \frac{4}{3} \left( \frac{\cos \phi}{E(\phi)} - \frac{(1-a^2/b^2) \sin^2 \phi \cos \phi}{[E(\phi)]^2} \right) Z = \frac{4}{3}. \tag{18}$$

At the uppermost point on the cylinder where  $\phi = 0$ ,  $z$  is continuous, smooth and  $\partial Z/\partial \phi = 0$ . Hence equation (18) reduces to

$$\frac{\partial Z(X, \phi = 0)}{\partial X} = \frac{4}{3} \left( 1 - \frac{b^2}{a^2} Z \right). \tag{19}^*$$

Integrating equation (19) gives

$$Z(X, \phi = 0) = \left( \frac{a}{b} \right)^2 \left[ 1 - \exp \left( -\frac{4}{3} \frac{b^2}{a^2} X \right) \right] + f(\phi). \tag{20}$$

Using the boundary condition, equation (15) we find that  $f(\phi) = 0$ . Hence, for the dimensionless film thickness,  $Z$ , at the uppermost part of the cylinder, we can write

$$Z(X, \phi = 0) = \left( \frac{a}{b} \right)^2 \left[ 1 - \exp \left( -\frac{4}{3} \frac{b^2}{a^2} X \right) \right]. \tag{21}$$

Further modification of equation (13), obtained by designating  $a = b = r$ , leads to

$$\frac{\partial Z}{\partial X} + \sin \phi \frac{\partial Z}{\partial \phi} + \frac{4}{3} \cos \phi Z = \frac{4}{3}. \tag{22}$$

Equation (22) is identical to the differential equation obtained by Hassan and Jakob [8] who investigated the problem of laminar film condensation on inclined circular cylinders.

2. *Horizontal elliptical and circular cylinders*

When  $R = \infty$  and  $\alpha = 0$ , equation (12) will reduce to

$$\frac{\sin \phi dZ}{E(\phi) d\phi} + \frac{4}{3} \left( \frac{\cos \phi}{E(\phi)} - \frac{(1-a^2/b^2) \sin^2 \phi \cos \phi}{[E(\phi)]^2} \right) Z = 4/3. \tag{23}$$

\* Hassan and Jakob [8] employed this scheme to evaluate the film thickness at the uppermost part of inclined circular cylinders.

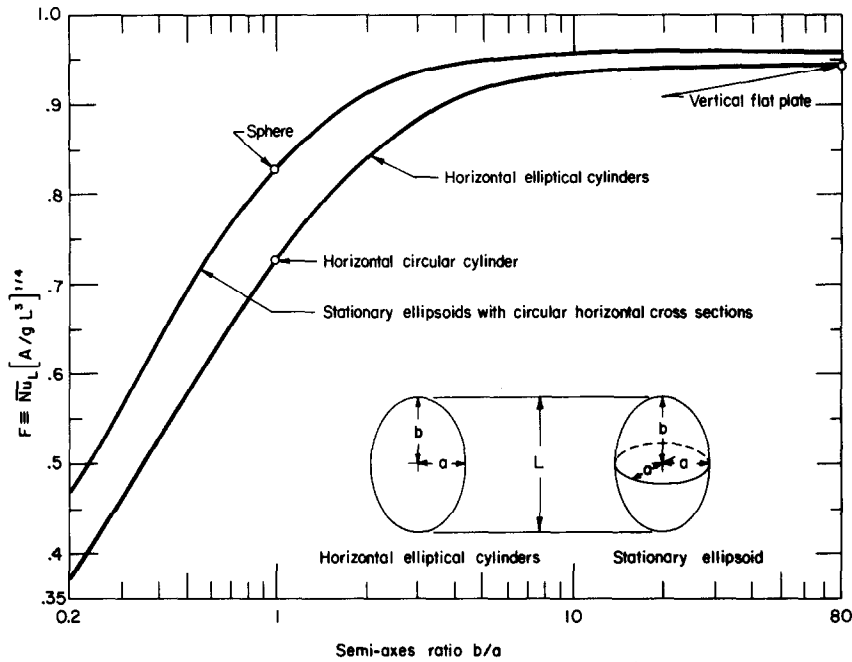


FIG. 4. Average Nusselt number for laminar film condensation.

At the uppermost part of the cylinder where  $\phi = 0$ ,  $Z$  is continuous and smooth, so  $dZ/d\phi = 0$ . In this case  $X$  is a constant approaching infinity, and equation (21) gives

$$Z(\phi = 0) = a^2/b^2. \quad (24)^*$$

For various ratios of  $b/a$ , equation (23) was evaluated numerically and the resulting values of  $h$ , obtained from equation (17), were averaged over the circumference of the cylinder. The results were used to evaluate the values of  $\overline{Nu}_L/(gL^3/A)^{1/4} = F$  which are plotted in Fig. 4. In this case the characteristic length,  $L$ , is taken to be equal to  $2b$ .

Figure 4 shows that at one extreme the value of  $F$  asymptotically approaches the value of 0.943 as the ratio of  $b/a$  increases to a value much greater than unity (vertical plates), as obtained by the Nusselt-Rohsenow analysis. When  $a/b = 1$  the value of  $F$  approaches 0.728 corresponding to the case of a horizontal circular cylinder.

3. Inclined flat plate

For  $R = \infty$  and  $b = 0$ , equation (12) reduces to that of condensation on a flat plate, inclined with angle  $\alpha$  from the horizontal, obtained by the Nusselt-Rohsenow analysis. The average Nusselt number based on the length of the flat plate is given by

$$\overline{Nu}_L = 0.943 \left( g \sin \alpha \frac{L^3}{A} \right)^{1/4}. \quad (25)$$

4. Stationary ellipsoids of circular horizontal cross sections and spheres

When  $R = 0$  and  $\alpha = 0$ , equation (12) is reduced to

$$\frac{\sin \phi dZ}{E(\phi)} + \frac{4}{3} \left( \frac{2 \cos \phi (1 - a^2/b^2) \sin^2 \phi \cos \phi}{[E(\phi)]^2} \right) Z = \frac{4}{3}. \quad (26)$$

\*This will replace the assumption that film thickness is zero at upper stagnation point used in most Nusselt-Rohsenow analyses.

Applying the conditions of continuity and smoothness of  $Z$  at the upper stagnation point,  $dZ/d\phi = 0$ , where  $\phi = 0$ , we obtain from equation (26)

$$Z(\phi = 0) = \frac{1}{2}(a/b)^2. \quad (27)$$

Equation (26) for various ratios of  $b/a$  was numerically evaluated. The resulting values of  $h$  were averaged over the entire surface of the ellipsoids. The corresponding values of  $F$  are plotted in Fig. 5, where the characteristic length,  $L$ , is equal to  $2b$ .\*

The special cases considered thus far were not influenced by induced centrifugal forces in the condensate film. We shall now consider a case in which the influence of centrifugal forces must be accounted for.

5. Helical circular cylinders

Substituting  $a = b = r$ , we get from equation (13)

$$\begin{aligned} \frac{\partial Z}{\partial X} + \left[ \sin \phi \left( 1 + \frac{d}{D} \sin \phi \right) + \frac{7}{9} \frac{d}{D} B \cos Z \right] \frac{\partial Z}{\partial \phi} \\ + \frac{4}{3} \cos \phi \left( 1 + 2 \frac{d}{D} \sin \phi \right) Z - \frac{4}{9} \frac{d}{D} B \sin \phi Z^2 \\ = \frac{4}{3} \left( 1 + \frac{d}{D} \sin \phi \right) \end{aligned} \quad (28)$$

subject to the boundary condition

$$Z(X = 0, \phi) = 0. \quad (15)$$

For inclined circular cylinders Hassan and Jakob [8] showed that for  $X \geq 3.2$  the thickness of the condensate film approximately approaches its limit at

\*The value of the average Nusselt number for laminar film condensation on spheres in this work exceeds those obtained in [9] and [10] by 5.2% and 3%, respectively. The discrepancy is a result of an erroneous definition of the average heat-transfer coefficient in [9] and [10]. In this report the values of  $F$  for the upper stagnation point and the upper hemisphere are found to be equal to 1.075 and 0.985, respectively.

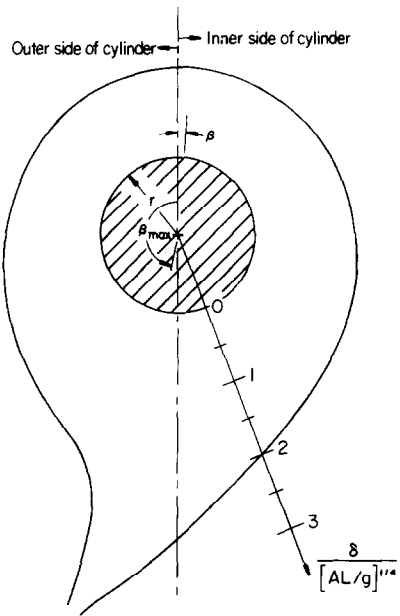


FIG. 5. Condensate film thickness on a helical circular cylinder:  $d/D = 0.2$  and  $B = 0.04$ .

$X = \infty$ . Hence for circular cylinders when  $X > 3.2$ , the  $X$  dependency of the film thickness can be ignored.

In the case under consideration the condensate film in the developing region ( $X < 3.2$ ) is absolutely thin as compared with the film thickness at  $X = \infty$ , in particular on the underside of the cylinder where the centrifugal forces are most effective. Therefore when the centrifugal effect can be ignored ( $B = 0$ ), numerical evaluation of equation (28) indicates that the condensate film thickness again approaches a limit when  $X \geq 3.2$ . Then equation (13) reduces to

$$\left[ \sin \phi \left( 1 + \frac{d}{D} \sin \phi \right) + \frac{7}{9} \frac{d}{D} B \cos \phi Z \right] \frac{dZ}{d\phi} + \frac{4}{3} \cos \phi \left( 1 + \frac{2d}{D} \sin \phi \right) Z - \frac{4}{9} \frac{d}{D} B \sin \phi Z^2 = \frac{4}{3} \left( 1 + \frac{d}{D} \sin \phi \right). \quad (29)$$

The L.H.S. bracket in equation (29) is zero, at a point on the cylinder, when  $\phi = \beta$  and the dimensionless film thickness,  $Z(\beta)$ , is

$$Z(\beta) = -(9/7) \frac{\tan \beta}{Bd/D} \left( 1 + \frac{d}{D} \sin \beta \right) \quad (30)$$

substituting equation (30), equation (29) can be written as

$$49B \frac{d}{D} \cos^2 \beta + 63 \sin \beta \cos^2 \beta \left( 1 + 2 \frac{d}{D} \sin \beta \right) + 27 \sin^2 \beta \left( 1 + \frac{d}{D} \sin \beta \right) = 0. \quad (31)$$

For determining the upper polar stagnation point ( $\beta$ ) on the cylinder, equation (31) was numerically solved for practical values of  $d/D$  and  $B$ . The results were used to evaluate the respective dimensionless film thickness at the upper polar stagnation point,  $Z(\beta)$ , from equation (30).

The results of these numerical calculations are summarized in Table 1. The ratio of  $d/D$  varies in the range of zero to 0.5, and the dimensionless group  $B$  varies between zero and 1. Values of  $B$  greater than unity are not considered since the analysis is restricted to  $C_p \Delta T / h_{fg} \leq 1$ , and  $Pr \geq 1$ . To ignore the effect of the starting region on the average heat-transfer coefficient, the helix angle  $\alpha$  cannot be much greater than  $45^\circ$ . Table 1 also presents the polar angle  $\beta_{max}$  at which the film thickness is maximum.

A study of Table 1 indicates that due to the effect of centrifugal forces exerted on the condensate film, the film thickness is not symmetrical with respect to the  $x_3$  axis, since the condensate film is much thicker on the under than on the upper side of the cylinder. Another observation is that the upper polar stagnation point and the location of the maximum film thickness increasingly deviates from polar angles  $\phi = 0$  and  $\phi = \pi$  respectively, with increasing  $d/D$  and  $B$ .

The dimensionless film thickness  $\delta / (AL/g)^{1/4}$  on a helical circular cylinder with ratios of diameters  $d/D = 0.2$  and typical value of  $B = 0.04$ , is presented in Fig. 5. The film thickness is greatly exaggerated for clarity, and the characteristic length,  $L$ , is taken to be equal to  $d/\cos \alpha$ . Figure 5 clearly shows the asymmetrical effect of centrifugal forces on the condensate film.

The restriction that no liquid is added by dropping from adjacent upper level of tubing to the condensate on the surface of the cylinder is satisfied when

$$\beta_{max} < \pi - \sin^{-1} \left( 0.1592 \frac{d}{D \tan \alpha} \right). \quad (32)$$

Hence for practical applications  $\beta_{max}$  from Table 1 should be checked with equation (32).

Equation (29) was numerically evaluated for practical values of  $d/D$  and  $B$ , and the resulting values of  $h$  averaged over the surface of the cylinder. The average Nusselt number  $\overline{Nu}_L / (gL^3/A)^{1/4} = F$ , for values of  $d/D$  from zero to 0.7 is shown in Fig. 6, with the centrifugal relation  $B$  taken as a constant parameter. For  $d/D = 0$

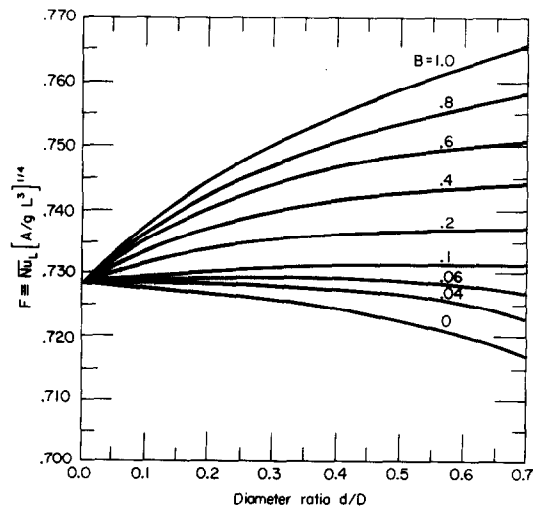


FIG. 6. Average Nusselt number for laminar film condensation on helical circular cylinders.

Table 1. Upper and lower polar stagnation points and the film thickness at upper stagnation for laminar film condensation on the helical circular cylinders

| B    | d/D = 0.1     |              |                     |               | d/D = 0.2     |              |                     |               | d/D = 0.3     |              |                     |               | d/D = 0.4     |              |                     |               | d/D = 0.5     |              |                     |               |
|------|---------------|--------------|---------------------|---------------|---------------|--------------|---------------------|---------------|---------------|--------------|---------------------|---------------|---------------|--------------|---------------------|---------------|---------------|--------------|---------------------|---------------|
|      | $\beta^\circ$ | Z( $\beta$ ) | $\beta_{max}^\circ$ | $\beta_{max}$ | $\beta^\circ$ | Z( $\beta$ ) | $\beta_{max}^\circ$ | $\beta_{max}$ | $\beta^\circ$ | Z( $\beta$ ) | $\beta_{max}^\circ$ | $\beta_{max}$ | $\beta^\circ$ | Z( $\beta$ ) | $\beta_{max}^\circ$ | $\beta_{max}$ | $\beta^\circ$ | Z( $\beta$ ) | $\beta_{max}^\circ$ | $\beta_{max}$ |
| 0.00 | 0.000         | 1.000        | 180.00              | 180.00        | 0.000         | 1.000        | 180.00              | 180.00        | 0.000         | 1.000        | 180.00              | 180.00        | 0.000         | 1.000        | 180.00              | 180.00        | 0.000         | 1.000        | 180.00              | 180.00        |
| 0.02 | -0.089        | 1.000        | 171.49              | 168.47        | -0.179        | 1.001        | 166.26              | 166.26        | -0.268        | 1.001        | 166.26              | 166.26        | -0.358        | 1.003        | 164.50              | 164.50        | -0.449        | 1.004        | 163.04              | 163.04        |
| 0.04 | -0.178        | 1.000        | 168.66              | 164.78        | -0.357        | 1.001        | 164.78              | 162.03        | -0.538        | 1.003        | 162.03              | 162.03        | -0.720        | 1.005        | 159.91              | 159.91        | -0.906        | 1.008        | 159.20              | 159.20        |
| 0.06 | -0.268        | 1.001        | 166.62              | 162.15        | -0.537        | 1.002        | 162.15              | 159.06        | -0.809        | 1.004        | 159.06              | 159.06        | -1.086        | 1.008        | 156.72              | 156.72        | -1.369        | 1.012        | 154.86              | 154.86        |
| 0.08 | -0.357        | 1.001        | 164.96              | 160.05        | -0.717        | 1.003        | 160.05              | 156.71        | -1.082        | 1.006        | 156.71              | 156.71        | -1.451        | 1.010        | 154.21              | 154.21        | -1.841        | 1.017        | 152.26              | 152.26        |
| 0.10 | -0.446        | 1.001        | 163.54              | 158.27        | -0.897        | 1.003        | 158.27              | 154.74        | -1.356        | 1.007        | 154.74              | 154.74        | -1.829        | 1.013        | 152.12              | 152.12        | -2.321        | 1.021        | 150.09              | 150.09        |
| 0.20 | -0.894        | 1.002        | 158.34              | 151.85        | -1.805        | 1.007        | 151.85              | 147.71        | -2.751        | 1.015        | 147.71              | 147.71        | -3.758        | 1.028        | 144.75              | 144.75        | -4.859        | 1.047        | 142.52              | 142.52        |
| 0.30 | -1.343        | 1.002        | 154.66              | 147.44        | -2.724        | 1.010        | 147.44              | 142.95        | -4.188        | 1.023        | 142.95              | 142.95        | -5.801        | 1.045        | 139.82              | 139.82        | -7.673        | 1.078        | 137.50              | 137.50        |
| 0.40 | -2.245        | 1.004        | 149.27              | 141.12        | -4.596        | 1.017        | 141.12              | 136.27        | -5.669        | 1.032        | 136.27              | 136.27        | -7.975        | 1.063        | 136.05              | 136.05        | -10.856       | 1.117        | 133.67              | 133.67        |
| 0.50 | -2.698        | 1.005        | 147.14              | 138.67        | -5.549        | 1.021        | 138.67              | 133.70        | -7.196        | 1.042        | 133.70              | 133.70        | -10.298       | 1.085        | 132.97              | 132.97        | -14.549       | 1.167        | 130.56              | 130.56        |
| 0.60 | -3.152        | 1.006        | 145.25              | 136.52        | -6.512        | 1.025        | 136.52              | 131.47        | -8.770        | 1.052        | 133.70              | 133.70        | -12.793       | 1.109        | 130.36              | 130.36        | -18.989       | 1.235        | 127.93              | 127.93        |
| 0.70 | -3.607        | 1.007        | 143.54              | 134.61        | -7.487        | 1.029        | 134.61              | 129.49        | -10.393       | 1.062        | 131.47              | 131.47        | -15.483       | 1.136        | 128.09              | 128.09        | -24.539       | 1.329        | 125.65              | 125.65        |
| 0.80 | -4.063        | 1.008        | 141.99              | 132.87        | -8.472        | 1.033        | 132.87              | 127.71        | -12.067       | 1.073        | 129.49              | 129.49        | -18.387       | 1.167        | 126.09              | 126.09        | -31.406       | 1.451        | 123.63              | 123.63        |
| 0.90 | -4.520        | 1.008        | 140.55              | 131.29        | -9.467        | 1.037        | 131.29              | 126.09        | -13.791       | 1.085        | 127.71              | 127.71        | -21.516       | 1.201        | 124.30              | 124.30        | -38.303       | 1.557        | 121.82              | 121.82        |
| 1.00 |               |              |                     |               |               |              |                     |               | -15.565       | 1.098        | 126.09              | 126.09        | -24.852       | 1.238        | 122.67              | 122.67        | -43.515       | 1.601        | 120.18              | 120.18        |

the value of  $F$  agrees with Hassan and Jakob's results for laminar film condensation on the inclined circular cylinders. For diminishing value of  $B$ , the effect of the centrifugal forces are negligible and the configuration factor,  $d/D$  has the dominant influence on the condensate film. Therefore, the average Nusselt number decreases slightly with increasing configuration factor  $d/D$ .\* However, for larger values of  $B \geq 0.1$ , the centrifugal forces have the dominant effect on the condensate film. Hence increasing  $d/D$  results in a continuous increase of the average Nusselt number. The values of  $F$  in Fig. 6 are again restricted to condensers with  $X_L \geq 50$ , so that the neglect of film development distance does not influence the over-all heat-transfer prediction.

Keeping the physical properties, the diameter of the cylinder  $d$ , and the angle of inclination  $\alpha$ , constant and letting the values of  $d/D$  and  $B$  vary, the average Nusselt number  $\overline{Nu}_L$ , evaluated in this report lies within 8.5% of that for an inclined cylinder.

It should be pointed out that we have only touched upon the problem of condensation on helical circular cylinders. A number of problems still remain. Like all previous well established condensing systems (flat plates, horizontal cylinders, spheres) for  $Pr \ll 1$  the inertia forces cannot be ignored and when  $C_p \Delta T / h_{fg}$  is large the film can become ripply or turbulent. There is insufficient experimental or analytical data available for comparison with the values obtained. The only data known to us are those for condensation on inclined cylinders in [8].

CONCLUSIONS

1. The governing equations for condensing flow have been formulated for helical elliptical cylinders. It has been shown that the appearance of non-linear terms in these equations is a result of centrifugal forces exerted on the condensate film.
2. The centrifugal effect can be disregarded for diminishing values of either  $a/R$  or  $B$ .
3. The solution for the governing differential equations yields an average Nusselt number expressed as

$$\overline{Nu}_L = F [gL^3/A]^{1/4}$$

where  $F$  varies with the configuration and centrifugal parameters as shown in Figs. 4 and 6.

\*Dhir and Lienhard [9] developed the following expression for Nusselt number for laminar film condensation of axisymmetric bodies in nonuniform gravity:

$$Nu = 0.707 \left( g_{eff} \frac{x^3}{A} \right)^{1/4}$$

where

$$g_{eff} = \frac{x[g(x)R(x)]^{4/3}}{\int_0^x [g(x)]^{1/3} [R(x)]^{4/3} dx}$$

for doughnut shaped circular cylinders (cylinder diameter  $d$  and doughnut diameter  $D$ ),  $x = (d/2)\phi$ ,  $g(x) = g \sin \phi$ ; and  $R(x) = (D/2)(1 + d \sin \phi/D)$ , this expression gives Nusselt numbers, which, when averaged over the entire surface of the cylinders, are identical to Fig. 6 for the value of  $B = 0$ .

4. The present investigation enables the design of helical reflux condensers for common liquids without serious computational difficulty.

*Acknowledgements*—The author wishes to thank Prof. J. Lienhard for suggesting the problem and is grateful to Profs. Lienhard and Eichhorn for providing guidance and suggestions during the investigation and preparation of this report.

The financial support provided by the Graduate School and the Department of Mechanical Engineering at the University of Kentucky is also gratefully acknowledged.

#### REFERENCES

1. W. Nusselt, Die Oberflächenkondensation des Wasserdampfes, *Z. Ver D. Ing.* **60**, 541–546; 569–575 (1916).
2. L. A. Bromley, Effect of heat capacity of condensate, *Ind. Engng Chem.* **44**, 2966–2968 (1952).
3. W. M. Rohsenow, Heat transfer and temperature distribution in laminar film condensation, *J. Heat Transfer* **78C**, 1645–1648 (1956).
4. E. M. Sparrow and J. L. Gregg, A boundary layer treatment of laminar film condensation, *J. Heat Transfer* **81C**(1), 13–18 (1959).
5. E. M. Sparrow and J. L. Gregg, Laminar condensation heat transfer on a horizontal cylinder, *J. Heat Transfer* **81C**(3), 291–296 (1959).
6. M. M. Chen, An analytical study of laminar film condensation. Part I—Flat plates, *J. Heat Transfer* **83C**(1), 48–55 (1961).
7. J. C. Y. Koh, E. M. Sparrow and J. P. Hartnett, The two phase boundary layer in laminar film condensation, *Int. J. Heat Mass Transfer* **2**, 69–82 (1961).
8. K. Hassan and M. Jakob, Film condensation of pure saturated vapors on inclined circular cylinders, *J. Heat Transfer* **80**, 887–894 (1958).
9. V. K. Dhir and J. H. Lienhard, Laminar film condensation on plane and axisymmetric bodies in non-uniform gravity, *J. Heat Transfer* **93C**, 97–100 (1971).
10. J. W. Yang, Laminar film condensation on a sphere, *J. Heat Transfer*, **95C**, 174–178 (1973).

### CONDENSATION EN FILM LAMINAIRE SUR DES CONDENSEURS HELICOIDaux ET CONFIGURATIONS ASSOCIEES

**Résumé**—Par la méthode de Nusselt–Rohsenow on analyse la condensation en film laminaire sur des cylindres elliptiques et hélicoïdaux. La formulation inclut les forces locales centrifuges et gravitationnelles. On présente une équation différentielle adimensionnelle et les paramètres sans dimension liés à la configuration et à la centrifugation sont identifiés. On traite une variété de systèmes et en particulier divers cylindres circulaires hélicoïdaux et semi-infinis. Les résultats de transfert thermique sont ensuite présentés et discutés. Dans toutes les situations pratiques (à l'exclusion de la condensation des métaux liquides), les coefficients moyens de transfert thermique à la condensation sur des cylindres circulaires, hélicoïdaux et semi-infinis, s'approchent à moins de 8,5% des valeurs pour les cylindres circulaires et inclinés.

### LAMINARE FILMKONDENSATION IN GEWENDELTEN RÜCKLAUF-KONDENSATOREN UND ÄHNLICHEN ANORDNUNGEN

**Zusammenfassung**—Die laminare Filmkondensation an gewendelten elliptischen Zylindern wird mit Hilfe der Nusselt–Rohsenow-Methode untersucht. Es wird eine allgemeine dimensionslose Differentialgleichung aufgestellt und auf dimensionslose Parameter eingegangen. Eine Vielzahl von Kondensationsystemen—insbesondere verschiedene halbunendliche, gewendelte Kreiszyylinder—wird untersucht. Wärmeübergangsergebnisse werden angegeben und diskutiert. Die mittleren Wärmeübergangskoeffizienten für die Kondensation an halbunendlichen, gewendelten Kreiszyindern liegen für alle praktischen Fälle (außer für die Kondensation von Metallen) innerhalb einer Abweichung von 8,5% von den für geneigte Kreiszyylinder gültigen Werte.

### ЛАМИНАРНАЯ ПЛЕНОЧНАЯ КОНДЕНСАЦИЯ НА ПОВЕРХНОСТЯХ ДЕФЛЕГМАТОРОВ СПИРАЛЕВИДНОЙ ФОРМЫ И АНАЛОГИЧНЫХ КОНФИГУРАЦИЙ

**Аннотация**—С помощью метода Нуссельта–Розенау анализируется ламинарная пленочная конденсация на поверхностях спиралевидных эллиптических цилиндров. Постановка задачи включает рассмотрение как локальных центробежных, так и гравитационных сил. Представлено общее дифференциальное уравнение в безразмерном виде и выделены безразмерные параметры, характеризующие центробежные силы и конфигурацию. Рассматривается множество конденсирующих систем, в частности, различные полубесконечные спиралевидные круговые цилиндры. Наконец, представлены и обсуждаются данные по теплообмену. Во всех практических ситуациях (исключая конденсацию жидких металлов) отличие средних значений коэффициентов теплообмена для конденсации на поверхностях полубесконечных спиралевидных круговых цилиндров от значений, полученных для наклонных круговых цилиндров, составляет 8,5%.